ISSN: 0067-2904

Secure and Robust Watermarking Using NSST-LWT-DCT-SVD for Copyright Protection

Siti Nur Avivah[1], Ferda Ernawan[1,2*]
[1]*Faculty of Computing, University Malaysia Pahang Al-Sultan Abdullah, Pekan, Malaysia*
[2]*Faculty of Information Technology, Universitas Nusa Mandiri, Indonesia*

Received: 19/5/2024 Accepted: 7/7/2025 Published: 30/10/2025

Abstract

The ongoing issue of unauthorized image distribution poses a serious modern challenge. This research introduces an innovative dual image watermarking technique that determines a potential embedding area in a small 4×4 DCT block and employs a hybrid approach of NSST-LWT-DCT-SVD to ensure efficient copyright protection. The watermark images are integrated using the red and green channels. These channels are then transformed using NSST-LWT to extract the low-frequency sub-band. Following this, the low-frequency section is divided into 4×4 blocks. The Human Visual System (HVS) is then used to select the appropriate blocks, which are transformed using DCT. Certain coefficients from the middle frequency of the DCT are chosen for decomposition with SVD. The singular values are then employed for embedding the watermark bits. Experimental results indicate that the proposed technique is a viable option for image watermarking, achieving average PSNR and SSIM values of up to 45.9 dB and 0.9962, respectively, while closely approaching a value of 1 for NC performance.

Keywords: Image watermarking, NSST, lifting wavelet transform, DCT, new embedding region.

1. Introduction

The widespread availability of mobile phones and digital cameras has led to an explosion of digital content creation and sharing. While this has enriched our lives in many ways, it has also introduced significant challenges related to the security and integrity of the digital images. One notable concern is the susceptibility of content shared on social media platforms to breaches, indicating a growing risk of unauthorized access and misuse of digital images. This constant threat of digital data theft places content owners in a perpetual state of vulnerability, necessitating robust measures to safeguard against malicious actors. Addressing these challenges requires collaborative efforts from both industry and academia to develop and implement effective security solutions to protect digital images and preserve user privacy in the internet landscape.

*Email: ferda1902@gmail.com

Digital image watermarking is a fundamental tool for protecting digital images by embedding the encoding of an authenticity watermark into the carrier using such art rules that only authorized parties can access and decipher it. Image watermarking techniques can be classified based on various criteria [1]. Based on visibility, digital image watermarking can be visible or invisible. The visible watermarking technique adds watermarks in a way that they are easily perceptible to viewers [2]. These are generally used for branding or copyright purposes. While invisible watermarking is an embedded watermark in a manner that they are imperceptible to human eyes, it can be detected using specialized algorithms [3]. Based on the sensitivity, image watermarking is divided into robust and fragile watermarking. Robust watermarking is designed to make the watermark resistant to common image processing operations and attacks, such as compression, noise addition, or filtering [4]. While fragile watermarking is designed for the watermarks to be easily damaged or destroyed by any modification to the image, making them suitable for tamper detection and authentication [5]. Furthermore, based on the watermark embedding approach, image watermarking can be conducted in the spatial domain or the frequency domain [6]. Spatial domain watermarking incorporates the watermark into the pixel values of the image directly [7], [8]. In the frequency domain based, the watermark is embedded into specific frequency components of the image [9], [10]. This approach involves transforming the spatial representation of the image into the frequency domain using techniques such as the Discrete Fourier Transform (DFT) [11], [12] , Discrete Cosine Transform (DCT) [13], [14], Discrete Wavelet Transform (DWT) [15], [16], or other similar transforms. The frequency domain approach provides a more compact representation of the image and is robust against common image processing attacks while minimizing perceptual distortion.

This study introduces an innovative dual watermarking framework utilizing NSST-LWT-DCT-SVD alongside Arnold encryption and human visual system (HVS) considerations to determine the block embedding positions. Furthermore, novel embedding locations within the 4×4 DCT coefficients are identified. The optimal coefficients are denoted as C_1 and C_2. Both matrices is employed to extract the watermark. The proposed methodology demonstrates the capacity to attain superior invisibility and robustness against diverse manipulation attacks.

2. Related work

Duan et al [17] proposed a method for multiple image watermarking using NSST-DWT-SVD. The study involved utilizing 8 host images sized at 512×512 pixels, with a 32×32 binary watermark embedded within both the red and green channel images. In the red channel processing, the red image is computed by NSST-DWT-DCT. Subsequently, the LL sub-band was partitioned into 8×8-pixel blocks, a specific frequency range was chosen to form 2×2 as M_1 and M_2. These matrices were subjected to decomposition with SVD, the highest singular value is chosen to incorporate the watermark according to predefined rules. In the embedding process, a central image was employed to integrate the watermark. The green was cropped to extract the central area, followed by transformation through NSST-DWT. The LL sub-band was then split into 4×4 and computed by SVD. The highest singular value from this decomposition was utilized to incorporate the watermark bit based on specific rules. The study reported achieving high imperceptibility and robustness, with an average PSNR of up to 45 dB and an NC of 0.95.

Zhang et al [18] introduced a blind color image watermarking technique within the spatial domain using the direct current (DC) of the 2D Discrete Fourier Transform (2D-DFT). Their study involved employing 24-bit color images sized 512×512 sourced from the CVG-UGR and USC-SIPI databases, alongside two binary bit color watermark images, each measuring

32×32. Utilizing the Arnold transform, the researchers encrypted the watermark before insertion. Subsequently, the color image is split into its RGB channels, followed by subdivision of each channel into 2×2 blocks. A watermark bit was embedded into every pair of blocks by using a predetermined set of guidelines. Evaluation of this approach yielded an average PSNR of 40 dB and a Normalized Correlation (NC) coefficient of approximately 0.90. However, the study highlighted a slight reduction in resilience against cropping attacks.

2.1. NSST

The non-subsampled shearlet transform (NSST) is one of the variants of the shearlet transform that avoids subsampling (downsampling) the input image at each scale. The decomposition process in NSST involves two main components such as the NSLP and the Shearlet Filter. NSLP is responsible for capturing low-frequency information in the image and SF is for capturing directional information in the image. The combination of NSLP and SF components can provide a multi-scale, multi-directional representation of the input image. The NSST decomposition process involves the following steps which are defined by [19]:

1. Input image

$$I(x,y), \qquad x = 1,2,\dots,M; \qquad y = 1,2,\dots,N \tag{1}$$

where $M \times N$ = image size, and $I(x,y)$ = pixel image at location (x,y).

2. Apply Non-Subsampled Laplace Pyramid Filter (NSLP)

The NSLP decomposition splits the image into LL and LH, HL, HH sub-bands using a set of low-pass $h_L(n)$ and high-pass filters $h_H(n)$ with decomposition level (k).

$$LL_k(x,y) = \sum_m \sum_n h_L(m,n)\,.\, I(x-m, y-n) \tag{2}$$

$$LH_k(x,y) = \sum_m \sum_n h_H(m,n)\,.\, I(x-m, y-n) \tag{3}$$

$$HL_k(x,y) = \sum_m \sum_n h_H(n,m)\,.\, I(x-m, y-n) \tag{4}$$

$$HH_k(x,y) = \sum_m \sum_n h_H(n,m)\,.\, I(x-m, y-n) \tag{5}$$

3. Apply shearlet filter (SF)

$$S_{j,l}(x,y) = \sum_m \sum_n \psi_{j,l}(m,n)\,.\, LL_k(x-m, y-n) \tag{6}$$

where $S_{j,l}(x,y)$ = shearlet transformed coefficient at scale j and direction l; $\psi_{j,l}(m,n)$ = shearlet filter that controls directionality.

The shear matrix S_l is given by:

$$S_l = \begin{bmatrix} 1 & l \\ 0 & 1 \end{bmatrix} \tag{7}$$

with l = shearing parameter controlling the tilt of the shearlet.

4. Obtained NSST image

After decomposition, the NSST image is obtained. LL_k is the coarse approximation, and $S_{j,l}$ are the detailed sub bands in multiple directions.

$$NSST(I) = \{LL_k, S_{j,l}, S_{j,2}, \dots, S_{j,L}\} \tag{8}$$

This research used one level NSST to execute the image and select the low-frequency components for the embedding process.

3. Proposed Schemes

3.1. Embedding

The sequence of the embedding technique is shown in Figure 1 as detailed in Algorithms 1 and 2.

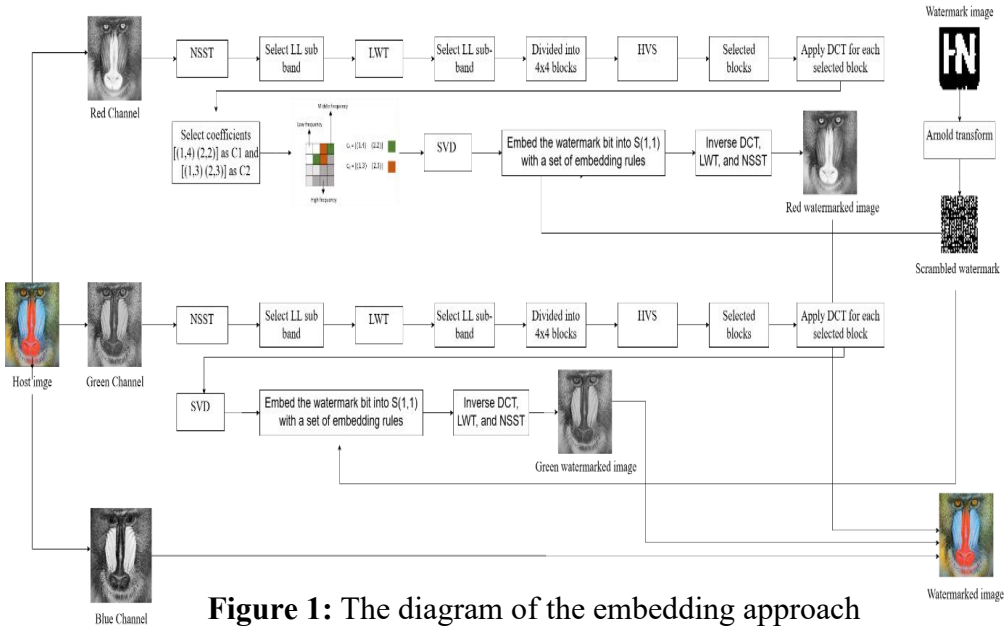

Figure 1: The diagram of the embedding approach

Embedding scheme for watermark 1

Step 1: Scrambled the watermark image using Arnold transform, then reshaped it to be one column.
Step 2: Separate the host image into RGB channels, then select the red channel.
Step 3: Transform the Red channel using one-level NSST to produce the LL component.
Step 4: Transform the LL component using a one-level 2D Lifting Wavelet.
Step 5: Select the LL component, then split it into a small block of 4×4.
Step 6: Determine the entropy of each block.
Step 7: Sorting the entropy and choosing the lowest values as the embedding area based on HVS.
Step 8: Transform each selected blocks using DCT.
Step 9: Select DCT coefficients as depicted in Figure 2 as matrix C_1 and C_2.
Step 10: Decompose matrix C_1 and C_2 using SVD.
Step 11: Select S (1,1) from each decomposed C_1 and C_2, then save them as S_1 and S_2, respectively.
Step 12: Compute average $S_1(1,1)$ and $S_2(1,1)$ then save it as E.
Step 13: Embed the watermark bit (W_b) using these equations:

$$S_1(1,1) = \begin{cases} E + T, & if\ W_b = 1 \\ E - T, & if\ W_b = 0 \end{cases} \qquad S_2(1,1) = \begin{cases} E - T, & if\ W_b = 1 \\ E + T, & if\ W_b = 0 \end{cases}$$

Step 14: Repeat Steps 8-13 until all watermark pixels are embedded.
Step15: Apply inverse DCT, LWT, and NSST to obtain the Red watermarked channel.

Embedding scheme for watermark 2

Step 1: Scrambled the watermark image using the Arnold transform and reshaped it to be one column.
Step 2: Select the green channel of the host image.
Step 3: Transform the green using NSST.
Step 4: Select the LL sub-band, then transform it using one level 2D-LWT.
Step 5: Divide the LL subband into a 4×4 non-overlapping block.
Step 6: Determine the embedding location blocks based on HVS.
Step 7: Transform the selected blocks using DCT.
Step 8: Decompose the block using SVD. The ($S_{(1,1)}$) is chosen for incorporating the watermark bit.
Step 9: Embed each binary watermark using the following rules:
Rule 1: Get δ value from modulus calculation between $S_{(1,1)}$ and Threshold (T).
Where the optimal Threshold (T) for this scheme is 319. $\delta = mod(S_{(1,1)}, T)$.
Rule 2: If the pixel value of the binary watermark = 0. $S_{(1,1)}$ is modified by:

$$S'_{(1,1)} = S_{(1,1)} - \delta + \left(\frac{1}{4}\right)T, where\ \delta \in [0.\left(\frac{3}{4}\right)T]$$

$$S'_{(1,1)} = S_{(1,1)} - \delta + \left(\frac{5}{4}\right)T, where\ \delta \in [\left(\frac{3}{4}\right)T, T]$$

Rule 3: If the pixel value of the binary watermark = 1, $S_{(1,1)}$ is modified by:

$$S'_{(1,1)} = S_{(1,1)} - \delta - \left(\frac{1}{4}\right)T, where\ \delta \in [0.\left(\frac{1}{4}\right)T]$$

$$S'_{(1,1)} = S_{(1,1)} - \delta + \left(\frac{3}{4}\right)T, where\ \delta \in \left[\left(\frac{1}{4}\right)T, T\right]$$

Step 11: Repeat steps 7-9 until all watermark bits are embedded.
Step 12: Apply invers LWT and NSST to obtain the green watermarked image.

3.2. Extraction

This section explains the extraction process of watermarked images. The flow diagram can be shown in Figure 2 and described in Algorithms 3 and 4. It needs a secret key to extract the watermark logo. In this research, the secret key is 10.

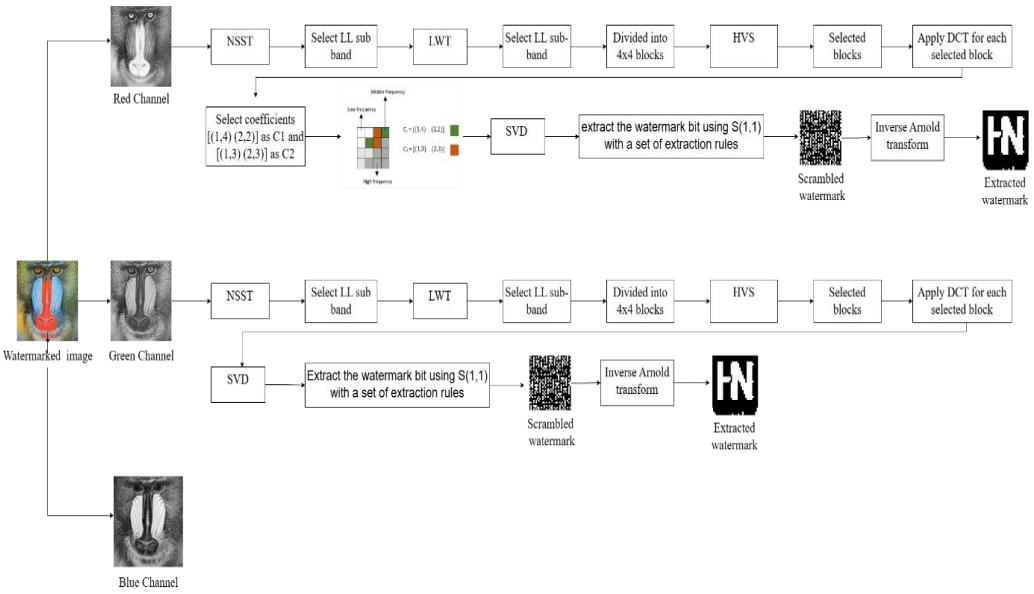

Figure 2: The Flow diagram of extracting approach.

Extraction process for watermark 1

Step 1: The image is divided into RGB channels.
Step 2: Transform the red channel with one level of NSST.
Step 3: Select the LL frequency of NSST, then perform 2D LWT.
Step 4: Divide the LL sub-band from the LWT matrices into a small block of 4×4.
Step 5: Calculate the entropy for each block.
Step 6: Sorting the entropy, then choose the blocks which have the lowest value based on HVS.
Step 7: The selected block is then transformed using DCT.
Step 8: Choose matrix C_1 and C_2 from the DCT coefficients.
Step 9: Decompose the matrices with SVD.
Step 10: Obtain the highest singular value of C_1 and C_2, then save it as $S_1'(1,1)$ and $S_2'(1,1)$.
Step 11: Extract the watermark by following the rules:

$$W_e' = \begin{cases} \text{watermark bits } = 1, if\ S_1'(1,1) > S_2'(1,1) \\ \text{watermark bits } = 0. if\ S_1'(1,1) < S_2'(1,1) \end{cases}$$

Step 12: Repeat step 7 until 11 to obtain the watermark.

Algorithm 4: Extraction process for watermark 2

Step 1: The image is separated into RGB.
Step 2: The green channel is then transformed by using one level of NSST.
Step 3: Transform the LL sub-band of NSST by using LWT.
Step 4: Divide the LL sub-band of LWT into 4×4 pixels.
Step 5: Calculate the entropy for each block.
Step 6: Sorting the entropy, then select the block which have the lowest value based on HVS.
Step 7: Transform the selected blocks with DCT.
Step 8: Decompose each DCT block using SVD.
Step 9: Obtain the highest singular value and save it as $S'(1, 1)$.
Step 10: Rule for extraction:
Rule 1: Calculate δ' by using this equation: $\delta' = \text{mod}(S'(1, 1), T)$. Where T is 339. It is a threshold that is obtained from a trade-off between robustness and imperceptibility.
Rule 2: Watermark bits (We') are obtained from this equation,
$We' = 0$. if $\delta' < (1/2)\ T$,
$We' = 1$, if $\delta' > (1/2)\ T$.
Step 11: Repeat step 7 until 10 to obtain the watermark.

4. Results

The proposed dual watermarking scheme was implemented on 12 host images and a binary watermark. The host images are obtained from USC-SIPI and Kodak databases. This scheme was conducted on the MATLAB platform version R2022a. The computations were carried out using a personal computer (PC) powered by Windows 10 Pro, a Core i5 CPU, and 8 GB of RAM. Figure 3 depicts the cover and watermark images. Furthermore, the achievement and comparison values of PSNR and SSIM are described in Tables 1 and 2. The robust strength is shown in Tables 3 and 4.

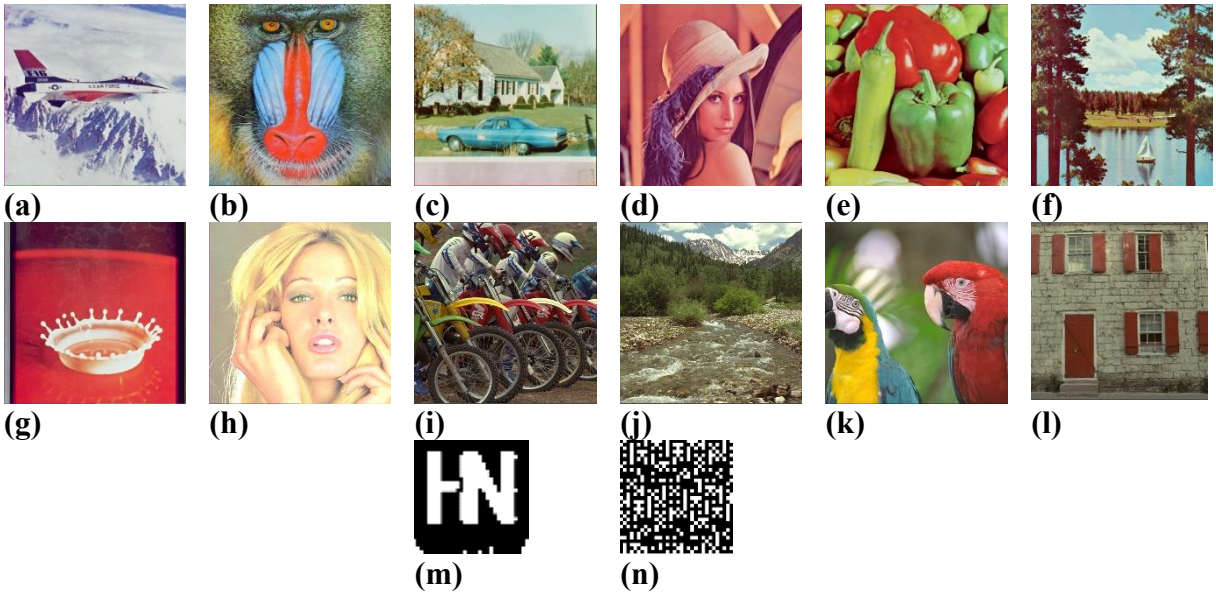

Figure 3: Cover images (a) Avion, (b) Baboon, (c) House, (d) Lena, (e) Peppers, (f) Sailboat, (g) Splash, (h) Tiffany, (i) Motocross, (j) Mountain, (k) two macaws, (l) stone building, (m) Binary watermark, and (n) Scrambled watermark.

Table 1: The invisibility and robustness performance without attack

No	Images	PSNR	SSIM	NC
1	Avion	42.1536	0.9838	0.9778
2	Baboon	41.7748	0.9956	0.9985
3	House	41.4112	0.9915	0.9896
4	Lena	43.4672	0.9855	0.9881
5	Peppers	43.6135	0.9877	0.9896
6	Sailboat	43.5342	0.9911	0.9970
7	Splash	43.8971	0.9814	0.9777
8	Tiffany	44.5932	0.9852	0.8923
9	Motocross	41.2092	0.9918	0.9896
10	Mountain	41.7207	0.9945	0.9956
11	Two macaws	41.3680	0.9850	0.9567
12	Stone building	43.4928	0.9921	0.9955
	Average	**42.6863**	**0.9888**	**0.9790**

Table 1 presents the imperceptibility evaluation for the suggested methodology. In this investigation, the average PSNR values are up to 42 dB, and the average SSIM is up to 0.98. These results collectively demonstrate that the proposed method generates high-quality watermarked images that effectively hide the watermark from human visual perception. On the other hand, to evaluate the quality performance of the proposed method, this research conducted a comparative analysis with prior experiments described in Table 2.

Table 2: Comparison of invisibility performance

No	Schemes	PSNR			SSIM		
		Lena	Peppers	Airplane	Lena	Peppers	Airplane
1	[18]	41.5249	39.9925	41.7434	0.9759	0.9761	0.9709
2	[20]	37.5851	38.0702	37.2966	0.9350	0.9241	0.9255
3	[21]	41.2219	40.7664	41.2226	0.9706	0.9650	0.9673
4	[22]	40.4747	41.4286	38.5970	0.9759	0.9817	0.9575
5	[23]	36.1046	34.6974	36.0268	0.9214	0.8951	0.9172
6	[24]	40.1061	40.1158	40.2973	0.9619	0.9624	0.9602
7	Proposed scheme	**43.4672**	**43.6135**	**42.1536**	**0.9855**	**0.9878**	**0.9838**

Table 2 illustrates a comparative analysis of imperceptibility performance between the proposed method and the advanced experiments conducted by [[18], [20], [21], [22], [23], [24]]. According to the findings presented in the table, the proposed approach demonstrates superiority over other comparative methods in terms of PSNR and SSIM across all tested images. Moreover, the proposed method achieves SSIM values close to 1, indicating a high similarity with the original images.

The effectiveness of the proposed methodology is assessed through a range of image processing and geometric adversities utilizing metrics such as Normalized Cross-Correlation (NC) and Bit Error Rate (BER). Additionally, this study conducted a comparative analysis of the proposed algorithm against other alternative image watermarking schemes.
Tables 3 and 4 illustrate a comparison of the proposed approach and [17] concerning Motocross, Mountain, and Baboon images with respect to signal processing and geometric attacks, respectively. Additionally, Figure 4 illustrates other comparative attacks.

Table 3: Comparison of NC based on signal processing attacks

No	Attacks	Motocross		Mountain		Baboon	
		[17]	Proposed scheme	[17]	Proposed scheme	[17]	Proposed scheme
1	Histogram equalization	0.9110	**0.9126**	0.9162	**0.9394**	0.9686	**0.9780**
2	Image brightens	0.9793	**0.9896**	0.9852	**0.9941**	0.9970	**0.9985**
3	Image darkens	0.9837	**0.9911**	0.9867	**0.9941**	0.9970	**0.9985**
4	Sharpening	0.9733	**0.9776**	0.9679	**0.9821**	0.9941	**1**
5	Gaussian noise (¦Ò= 0.1%)	0.9050	**0.9238**	0.9310	**0.9479**	0.9545	**0.9597**
6	Salt-pepper noise (den = 0.5%)	**0.9647**	0.9273	**0.9718**	0.9188	0.9091	**0.9318**
7	Speckle noise (0.1%)	0.9098	**0.9776**	0.9092	**0.9896**	0.9852	**0.9897**
8	Speckle noise (1%)	**0.9763**	0.8912	**0.9750**	0.8883	0.7954	**0.8723**
9	Poisson noise	0.9292	**0.9310**	0.8599	**0.9270**	0.8556	**0.9094**
11	Gaussian LPF 5×5	0.8785	**0.9821**	0.8602	**0.9822**	0.9970	**0.9985**

Table 4: Comparison of NC based on geometrical attacks

No	Attacks	Motocross		Mountain		Baboon	
		[17]	Proposed scheme	[17]	Proposed scheme	[17]	Proposed scheme
1	Non-Attack	0.9807	**0.9896**	0.9852	**0.9956**	0.9970	**0.9985**
2	JPEG (QF = 90%)	0.9779	**0.9881**	0.9838	**0.9941**	0.9970	**0.9985**
3	JPEG (QF = 80%)	0.9778	**0.9821**	0.9808	**0.9941**	0.9970	**0.9985**
4	JPEG (QF = 70%)	0.9719	**0.9866**	0.9792	**0.9881**	0.9956	**0.9970**
5	JPEG (QF = 60%)	0.9692	**0.9821**	0.9764	**0.9867**	0.9955	**0.9985**
6	JPEG (QF = 50%)	0.9674	**0.9791**	0.9633	**0.9881**	0.9941	**0.9955**
7	JPEG (QF = 40%)	0.9617	**0.9747**	0.9676	**0.9897**	0.9836	**0.9911**
8	Crop 25% (Upper right)	0.8364	**0.9896**	0.8520	**0.9956**	0.8514	**0.9985**
9	Crop 25% (bottom right)	0.8487	**0.9896**	0.8574	**0.9956**	0.8670	**0.9985**
10	Crop 50% (right half)	0.6919	**0.9896**	0.6955	**0.9956**	0.6992	**0.9985**
11	Scaling 0.8	0.8616	**0.9530**	0.8677	**0.9338**	0.9441	**0.9792**
12	Scaling 1.1	0.7919	**0.9281**	0.7986	**0.9035**	0.8885	**0.9342**
13	Scaling 1.2	0.8625	**0.9587**	0.8719	**0.9436**	0.9459	**0.9822**
14	Scaling 2	0.9778	**0.9881**	0.9823	**0.9896**	0.9970	**0.9985**

Table 3 illustrates the comparative robustness levels between the suggested method and [17] under various signal-processing attacks. In an analysis of the motocross image, the proposed method shows slightly less resilience against 0.5% salt-pepper noise, Poisson noise, and the 3×3 median filter. In contrast, the proposed approach shows greater resistance to all attacks applied to the mountain image, except for the 5×5 Gaussian LPF. Furthermore, regarding the Baboon image, the proposed method exhibits slightly lower robustness than [17] when subjected to Histogram equalization, Gaussian noise at 0.1%, 0.5% salt & pepper noise, the 3×3 median filter, and the 5×5 Gaussian LPF. In summary, the overall evaluation indicates that the proposed method surpasses [17] across all images compared.

Table 4 shows that the proposed approach exceeds the performance of [17] in all tested images and manipulation conditions, such as JPEG compression, cropping, and scaling. The proposed scheme gives a significant robustness value for cropping and scaling attacks. It can be concluded that the suggested embedding location in a compact 4×4 DCT block can improve the resilience of the watermarked images.

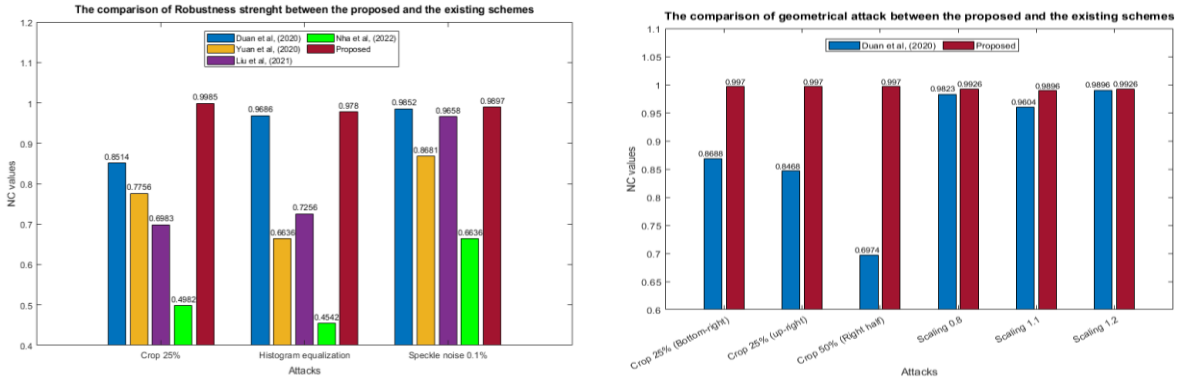

(a) **(b)**

Figure 4: The comparison of robustness strength between the proposed scheme and the existing scheme for watermark 2 (a) Baboon (b) Sailboat.

Figure 4 presents a comparison of resilience performance between the proposed approach and the existing methods. Specifically, Figure 4(a) emphasizes the improved resilience of the proposed method compared to others when subjected to cropping and histogram equalization attacks. In contrast, for the speckle noise attack, the proposed method exhibits a performance level that is comparable to [17]. Furthermore, Figure 4(b) demonstrates the marked superiority of the compared scheme. This is particularly evident in the substantial improvements noted across all cropping and scaling attacks, with an average NC value approaching 1.

5. Conclusion

To implement digital watermarking effectively for copyright protection, this study introduces a novel embedding location for a watermarking method using NSST-LWT-DCT-SVD. The LL frequency of NSST-LWT is split into 4×4. The selected blocks are subsequently processed by using DCT. The coefficients DCT of [(1,4); (2,2); (1,3); (2,3)] are chosen to embed the watermark. These selected coefficients are then processed by SVD decomposition. The highest singular value is then modified to incorporate the watermark bit following specific guidelines. Experimental results indicate that the proposed method achieves significant imperceptibility and robustness compared to existing approaches. The proposed scheme achieved PSNR up to 46 dB and SSIM of 0.99. While the NC performance is above 0.95. It is shown that the proposed algorithm satisfies the requirements for image watermarking. However, there are certain challenges that need to be tackled in the future, such as the need to adaptively adjust the embedding threshold based on image characteristics, which could further enhance robustness, particularly against noise and filtering attacks.

Acknowledgements

The authors would like to thank the Ministry of Higher Education for providing financial support under Universiti Malaysia Pahang Al-Sultan Abdullah under Internal Research Grant RDU233003.

References

[1] H. M. Al-Otum and A. A. A. Ellubani, "Secure and effective color image tampering detection and self restoration using a dual watermarking approach☆," *Optik (Stuttg)*, vol. 262, p. 169280, Jul. 2022, doi: 10.1016/j.ijleo.2022.169280.

[2] C. Fikri, F. A. Nugroho, B. Apriyansyah, and M. Fakhreldin, "Dual Watermarking Based on Human Visual Characteristics with IWT-SVD," IJACI : International Journal of Advanced Computing and Informatics, vol. 1, no. 1, pp. 1–12, Apr. 2025, doi: 10.71129/ijaci.v1.i1.pp1-12.

[3] R. Ridwan and M. N. Kabir, "Robust Color Image Watermarking Using Dual Embedding via Schur Decomposition," IJACI : International Journal of Advanced Computing and Informatics, vol. 1, no. 1, pp. 39–47, Apr. 2025, doi: 10.71129/ijaci.v1.i1.pp39-47.

[4] L. Zheng, Z. Li, R. Luo, Z. Liu, and C. Li, "VSTNet: Robust watermarking scheme based on voxel space transformation for diffusion tensor imaging images," *Journal of Information Security and Applications*, vol. 79, p. 103657, Dec. 2023, doi: 10.1016/j.jisa.2023.103657.

[5] X. Xia, S. Zhang, K. Wang, and T. Gao, "A novel color image tampering detection and self-recovery based on fragile watermarking," *Journal of Information Security and Applications*, vol. 78, p. 103619, Nov. 2023, doi: 10.1016/j.jisa.2023.103619.

[6] F. Y. Shih and S. Y. T. Wu, "Combinational image watermarking in the spatial and frequency domains," *Pattern Recognit*, vol. 36, no. 4, pp. 969–975, Apr. 2003, doi: 10.1016/S0031-3203(02)00122-X.

[7] X. Wang, R. Ma, Y. Shen, and P. Niu, "Image watermarking using DNST-PHFMs magnitude domain vector AGGM-HMT," *J Vis Commun Image Represent*, vol. 91, p. 103779, Mar. 2023, doi: 10.1016/j.jvcir.2023.103779.

[8] Z. Tang, X. Chai, Y. Lu, B. Wang, and Y. Tan, "An end-to-end screen shooting resilient blind watermarking scheme for medical images," *Journal of Information Security and Applications*, vol. 76, p. 103547, Aug. 2023, doi: 10.1016/j.jisa.2023.103547.

[9] S. Han, M. Lv, and Z. Cheng, "Dual-color blind image watermarking algorithm using the graph-based transform in the stationary wavelet transform domain," *Optik (Stuttg)*, vol. 268, p. 169832, Oct. 2022, doi: 10.1016/j.ijleo.2022.169832.

[10] R. Singh and A. Ashok, "An optimized robust watermarking technique using CKGSA in frequency domain," *Journal of Information Security and Applications*, vol. 58, p. 102734, May 2021, doi: 10.1016/j.jisa.2020.102734.

[11] Z. Xia *et al.*, "Geometric attacks resistant double zero-watermarking using discrete Fourier transform and fractional-order Exponent-Fourier moments," *Digit Signal Process*, vol. 140, p. 104097, Aug. 2023, doi: 10.1016/j.dsp.2023.104097.

[12] C. Qu, J. Du, X. Xi, H. Tian, and J. Zhang, "A hybrid domain-based watermarking for vector maps utilizing a complementary advantage of discrete fourier transform and singular value decomposition," *Comput Geosci*, vol. 183, p. 105515, Jan. 2024, doi: 10.1016/j.cageo.2023.105515.

[13] M. Begum, J. Ferdush, and M. S. Uddin, "A Hybrid robust watermarking system based on discrete cosine transform, discrete wavelet transform, and singular value decomposition," *Journal of King Saud University - Computer and Information Sciences*, vol. 34, no. 8, pp. 5856–5867, Sep. 2022, doi: 10.1016/j.jksuci.2021.07.012.

[14] F. Ernawan, D. Ariatmanto, and A. Firdaus, "An Improved Image Watermarking by Modifying Selected DWT-DCT Coefficients," *IEEE Access*, vol. 9, pp. 45474–45485, 2021, doi: 10.1109/ACCESS.2021.3067245.

[15] S. A. Nawaz, J. Li, M. U. Shoukat, U. A. Bhatti, and M. A. Raza, "Hybrid medical image zero watermarking via discrete wavelet transform-ResNet101 and discrete cosine transform," *Computers and Electrical Engineering*, vol. 112, p. 108985, Dec. 2023, doi: 10.1016/j.compeleceng.2023.108985.

[16] S. D. Mali and L. Agilandeeswari, "Non-redundant shift-invariant complex wavelet transform and fractional gorilla troops optimization-based deep convolutional neural network for video watermarking," *Journal of King Saud University - Computer and Information Sciences*, vol. 35, no. 8, p. 101688, Sep. 2023, doi: 10.1016/j.jksuci.2023.101688.

[17] S. Duan, H. Wang, Y. Liu, L. Huang, and X. Zhou, "A Novel Comprehensive Watermarking Scheme for Color Images," *Security and Communication Networks*, vol. 2020, pp. 1–12, Dec. 2020, doi: 10.1155/2020/8840779.

[18] X. Zhang, Q. Su, Z. Yuan, and D. Liu, "An efficient blind color image watermarking algorithm in spatial domain combining discrete Fourier transform," *Optik (Stuttg)*, vol. 219, p. 165272, Oct. 2020, doi: 10.1016/j.ijleo.2020.165272.

[19] S. N. Avivah, F. Ernawan, and A. F. Mat Raffei, "Dual image watermarking based on NSST-LWT-DCT for color image," *Indonesian Journal of Electrical Engineering and Computer Science*, vol. 35, no. 2, p. 907, Aug. 2024, doi: 10.11591/ijeecs.v35.i2.pp907-915.

[20] Z. Yuan, D. Liu, X. Zhang, and Q. Su, "New image blind watermarking method based on two-dimensional discrete cosine transform," *Optik (Stuttg)*, vol. 204, p. 164152, Feb. 2020, doi: 10.1016/j.ijleo.2019.164152.

[21] D. Liu, Q. Su, Z. Yuan, and X. Zhang, "A fusion-domain color image watermarking based on Haar transform and image correction," *Expert Syst Appl*, vol. 170, p. 114540, May 2021, doi: 10.1016/j.eswa.2020.114540.

[22] Q. Su, X. Zhang, and G. Wang, "An improved watermarking algorithm for color image using Schur decomposition," *Soft comput*, vol. 24, no. 1, pp. 445–460, Jan. 2020, doi: 10.1007/s00500-019-03924-5.

[23] D. Liu, Z. Yuan, and Q. Su, "A blind color image watermarking scheme with variable steps based on Schur decomposition," *Multimed Tools Appl*, vol. 79, no. 11–12, pp. 7491–7513, Mar. 2020, doi: 10.1007/s11042-019-08423-1.

[24] Q. Su, D. Liu, and Y. Sun, "A robust adaptive blind color image watermarking for resisting geometric attacks," *Inf Sci (N Y)*, vol. 606, pp. 194–212, Aug. 2022, doi: 10.1016/j.ins.2022.05.046.